Scientific Contributions Oil & Gas, Vol. 48. No. 1, April: 77 - 90

SCIENTIFIC CONTRIBUTIONS OIL AND GAS
Testing Center for Oil and Gas
LEMIGAS

Journal Homepage:http://www.journal.lemigas.esdm.go.id
ISSN: 2089-3361, e-ISSN: 2541-0520

Pore-Scale 3D Modeling of Viscous Fingering for Non-Newtonian Heavy Oil Recovery

Cindy Dianita[1,2], Muhammad Faturahman[1,2] and Andi Mardianza[3].

[1]Process Systems Engineering Laboratory, Faculty of Engineering, Universitas Indonesia
Lingkar street, Pondok Cina, Beji Sub-district, Depok City, West Java 16424, Indonesia

[2]Department of Chemical Engineering, Faculty of Engineering, Universitas Indonesia
Lingkar street, Pondok Cina, Beji Sub-district, Depok City, West Java 16424, Indonesia

[2]PT. Pertamina Hulu Energi, PHE Tower
TB Simatupang Street No.Kav. 99, South Jakarta, DKI Jakarta, Indonesia

Corresponding author: tmarhaendrajana@itb.ac.id.

Manuscript received: October 31th, 2024; Revised: December 20th, 2024
Approved: January 10th, 2025; Available online: April 08th, 2025.

ABSTRACT - Heavy oil recovery faces significant challenges due to the unstable displacement of oil by water, known as viscous fingering (VF). This occurs when low-viscosity fluids displace high-viscosity fluids, leading to inefficient oil recovery and increased water production. These issues reduce efficiency and increase environmental and economic costs, highlighting the need for improved simulation techniques to better understand and manage VF dynamics. This study examines the use of non-Newtonian Carreau fluids in modeling VF phenomena, offering more realistic simulations than Newtonian fluids. The shear-thinning behavior of Carreau fluids allows injected fluids to penetrate smaller pores effectively, influencing finger formation and growth. Current work, which incorporates non-Newtonian fluid characteristics, provides a more accurate representation of viscous fingering, including key features such as finger formation, merging, coalescence, blocking, tip-splitting, and expansion. Three porosity values (0.29, 0.5, and 0.7) are simulated to represent diverse reservoir conditions. A 3D computational fluid dynamics (CFD) model is utilized, employing the volume of fluid (VOF) approach to capture immiscible displacement processes. The model is validated using experimental data from coreflood studies. The results demonstrate that porosity significantly influences VF behavior, with lower porosities resulting in more pronounced finger formation, splitting, and coalescence. Non-Newtonian fluids decrease instability by moderating VF growth dynamics, enhancing displacement efficiency. These findings emphasize the importance of incorporating non-Newtonian fluid properties and porosity variations into VF simulations to optimize oil recovery processes. This study provides insights into VF dynamics, advancing the development of sustainable and efficient heavy oil recovery technologies.

Keywords: carreau fluid, computational fluid dynamics (CFD), non-newtonian fluid, porosity, viscous fingering.

How to cite this article:

Cindy Dianita, Muhammad Faturahman and Andi Mardianza, 2025, Pore-Scale 3D Modeling of Viscous Fingering for Non-Newtonian Heavy Oil Recovery, Scientific Contributions Oil and Gas, 48 (1) pp. 77-90. DOI.org/10.29017/scog.v48i1.1690.

INTRODUCTION

The constantly evolving oil and gas industry consistently innovates to improve profitability and sustainability in oil recovery. Despite these advancements, the industry faces significant challenges, especially the high production of water during oil recovery processes. This issue not only incurs substantial costs for water waste management but also impacts energy consumption and increases the carbon footprint of oil extraction operations (Temizel et al. 2018).

These challenges are exacerbated in heavy oil fields due to the high water-to-oil ratios. Heavy oil fields can sometimes produce up to 50 barrels of water per barrel of oil; however, typical water-oil ratios (WOR) can range between 5 and 6 barrels (Di Lullo & Rae 2002). While water generation is an unavoidable aspect of oil recovery, understanding the processes involved could lead to technological advancements that enhance productivity and reduce environmental impacts.

A significant phenomenon affecting water production in oil fields is viscous fingering (VF), which occurs when low-viscosity fluids are injected into a porous medium containing high-viscosity fluids. This results in the formation of finger-like patterns due to water's higher mobility compared to oil. The instability at the interface between the two fluids, characterized by finger-birth, tip splitting, side branching, and shielding, leads to the dominance of a few main fingers that channel the displacing water.

It has been shown by (Wang et al. 2023) that the size of the porosity has a great impact on the dynamics of VF. Porosity represents the measure of void spaces within a rock, determining its capacity to store and transmit fluids. In the context of heavy oil formations, porosity plays a dual role: influencing fluid flow dynamics, including oil recovery and water production, and affecting phenomena such as VF. It has also has been reported that mineral dissolutions can consume CO_2 and modify local porosity, hence affecting variations in fingering dynamics (Lei & Luo 2021).

While conventional reservoir simulations struggle to model these intricate dynamics due to computational limitations, advanced numerical techniques such as computational fluid dynamics (CFD) offer more precise modeling capabilities. Despite having been studied for several decades, most of the VF studies that have been conducted were performed on a microscale or even in 2D such as works from González & Asuaje 2014; Luo et al. 2017; Becker et al. 2018 and Singh et al. 2021). Recent advances have included three-dimensional (3D) experimental methods, and computational fluid dynamics (CFD) has shown promise in modelling this phenomenon. CFD offers advantages over traditional reservoir simulators by enabling the use of various mesh types and solving fluid flows near and in wells. CFD techniques have been employed to conduct numerical examinations at both pore-scale and continuum-scale levels. These models consider porosity explicitly, allowing for the investigation of how pore-scale heterogeneities influence VF behavior.

Heavy oil formations, characterized by their high viscosity (lower API gravity) and complex pore structures, present additional challenges when non-Newtonian fluids are used in recovery processes (Widarsono et al. 2021) such Duri field as the largest one, plays a very important role in making up the basin's whole oil production output. In general, the Central Sumatra Basin is also acknowledged for its heavy oil potential. Accordingly, a study under the auspices of the Ministry of Energy and Mineral Resources (MEMR. In contrast to Newtonian fluids, non-Newtonian fluids demonstrate shear-thinning or shear-thickening behaviour, which can markedly impact displacement processes and resulting morphologies. behaviorResearch has shown that shear-thickening fluids initially lag but eventually surpass Newtonian and shear-thinning fluids in finger patterns, highlighting their potential for enhanced oil recovery (Shi & Tang 2014; Sugihardjo et al. 2022; Tobing 2018).

This research is conducted based on the study by (Pinilla et al. 2021). From their research, it is revealed that the movement patterns of the fingers near the central surface or along its edge are similar to those commonly observed in Hele-Shaw displacements. Within the central region or the main body, the three-dimensional movements exhibit similar flow characteristics like merging, splitting, tip splitting, dominant fingers, and others. Despite the conclusions drawn from the research, this research aims to enhance simulations by incorporating the non-Newtonian viscosity model with Carreau Fluid, where previously it only utilizes the Newtonian model, into the simulation.

studyto createThis study investigates the impact of non-Newtonian fluid in the simulation to gain a deeper understanding of domain discretization effects in the 3D simulation of VF and its growth dynamics. In contrast to Newtonian fluids, non-Newtonian fluids may exhibit shear thinning or thickening behaviour, which can significantly affect the displacement process and the resulting morphologies. impactsshear-thinningbehaviorAccurate modeling of non-Newtonian fluids is necessary to capture these effects and obtain reliable predictions. modelingFurthermore, the volume of fluid physical model with the high-resolution capturing interface (HRCI) approach is used to simulate immiscible displacements of oil–water in core flood. The effect of porosity values is also assessed in terms of VF growth with 3 different values of VF (0.29, 0.5, and 0.7). The findings are confirmed by comparing them to data from experimental core flood experiments carried out by (Doorwar & Mohanty 2016).

By concentrating on these areas, this study aims to enhance the understanding of VF dynamics and contribute to the advancement of more efficient and environmentally sustainable oil recovery technologies.

METHODOLOGY

For this research, the CFD simulation data refers to the simulation of Pinilla et al. (2021) with isothermal assumption using shear-thinning Carreau fluid models from Montes et al. (2018). The simulation data required includes:Fluid properties (viscosity and density); Geometry used (diameter, length, and height); Fluid conditions (pressure, temperature, and flow rate).

The simulation parameters of this work are summarized in Table 1. The model validation data refers to (Doorwar & Mohanty's 2016) experimental study, and the reservoir simulator data used for comparing the numerical methods, CFD and reservoir simulation, is sourced from (Pinilla et al. 2021) research. Furthermore, after being validated, the data is analyzed in terms of its viscous fingering profile and pressure profile. Meanwhile, the geometry of this study is a vertical cylinder based on the geometry of (Pinilla et al. 2021) with a total length of 0.3048 m and a total diameter of 0.0508 m.

Table 1
Parameter of simulation

Parameter	Input
Model	Multiphase, Volume of Fluid (VOF), surface tension coefficient = 0.022 N/m Viscous: laminar
Water	Density = 998.2 kg/m^3, Viscosity = 0.001003 Pa.s
Heavy Oil	Density = 976 kg/m^3, Zero Shear Viscosity = 170.8 Pa.s, Infinite Shear Viscosity = 17.4 Pa.s
Operating Condition	P = 1.01325 x 10^5 Pa
Boundary Condition	Velocity of Water Inlet: 3.56 x 10^{-6} m/s, Porosity = 0.29, 0.5, and 0.7 Oil Volume Fraction = 0.95 Outlet: pressure outlet Wall: no-slip boundary condition
Control	Pressure-velocity coupling: SIMPLE Discretization Pressure: Second Order Upwind Momentum: Second Order Upwind Volume fraction : compressive
Residual	Absolute criteria Continuity = 0.001 X velocity = 0.001 Y velocity = 0.001 Z velocity = 0.001

RESULTS AND DISCUSSIONS

Grid independence test

The simulation work is initialized by conducting a grid independence test using 3 different mesh numbers. It is safe to say that this research can be conducted using a mesh with 326,181 number of elements due to the fact that it has a much smaller value of relative error in comparison with the other 2, with the value of relative error of pressure being 2.77% compared to the pressure results of the experimental result. Furthermore, the skewness, the orthogonality, and the aspect ratio of the mesh are reviewed to ensure the quality of the mesh. These mesh quality parameters indicate a good quality of the mesh of the selected number of elements with mesh configurations as shown in Figure 1.

Viscous fingering contour

Computational fluid dynamics (CFD) can simulate VF in 3D investigations using the porous media flow model, which is currently quite limited. This study not only fills this gap by demonstrating that CFD is more than capable of simulating VF development dynamics, but it also provides a qualitative comparison of fingering dynamics between CFD and the experiment conducted by Doorwar and Mohanty (2016). The 3D fingering growth will be examined on the core walls.

Figure 2 depicts the fingering at the walls, which is similar to the dynamics reported in the Hele-Shaw cell experiment theory. Figure 3 shows the results for up to 0.05 injected pore volume, which are compared to those found in the work of Pinilla et al. (2021). In this picture, the core wall is not seen in its cylindrical shape. Instead, it is projected as a plane to show the VF throughout the core circle.

The water-oil interface velocity after 500 seconds is displayed in Figure 4. This is in line with the water-oil interface's form seen in Figure 3. The velocity is low, roughly 10^{-5} m/s, which is comparable to displacement velocities typical in oil fields. The maximum velocity (U_{max}), which is approximately 1.64 x 10^{-5} m/s, is recorded at the central point beneath the wellbore. At locations farthest from the center, the interface's velocity drops, reaching a minimum velocity (U_{min}) of roughly 3.61 x 10^{-6} m/s. The graph of velocity in viscous fingering has a maximum and minimum point due to the dynamics of the displacement process. As the viscosity ratio between the displacing and displaced fluids increases, the initial minimum point of the velocity graph moves toward the injection point. As stated by Kargozarfard, Riazi, and Ayatollahi (2018), this phenomenon is a result of the unstable displacement of a more viscous fluid by a less viscous fluid, known as viscous fingering. The unstable nature of this displacement process results in the formation of maximum and minimum points on the velocity graph.

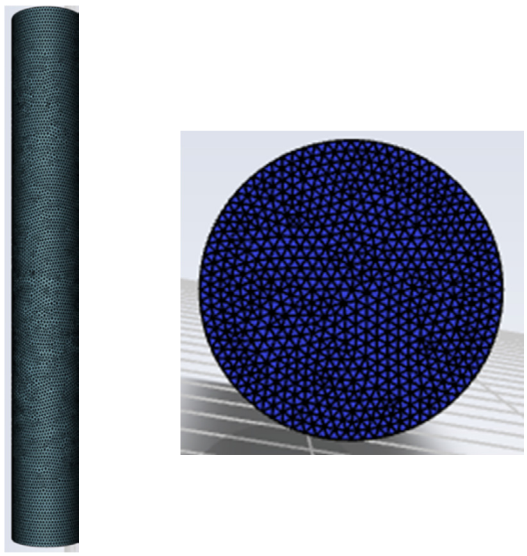

(a) (b)

Figure 1
Reservoir geometry model of this simulation work (a) vertical front view (b) cross-section of the mesh

 | DOI.org/10.29017/scog.v48i1.1690

It is also crucial to consider the effects of gravity on the creation of viscous fingering. The interaction between viscous finger motion and gravity plays a significant role in multiphase composite and compressible flows. According to Moortgat (2016), gravity can enhance finger flow in response to hydrophobization in highly permeable connecting regions. The presence of correlated inhomogeneities results in a transition from gravity-dominated flow to the viscosity-to-gravity ratio. Gravity and viscosity are the two fundamental forces that cause instability, and their dynamic effects cannot be substituted unless the interface is nearly flat and perpendicular to the motion. Hence, the connection between the behavior of viscous fingers and gravity is rooted in their individual impacts on the flow instability of the porous medium.

The two fundamental forces that cause instability are gravity and viscosity, and their dynamic effects cannot be replaced unless the interface is approximately flat and perpendicular to the motion. Therefore, the relationship between the behavior of the viscous fingers and gravity lies in their respective effects on the flow instability of the porous medium.

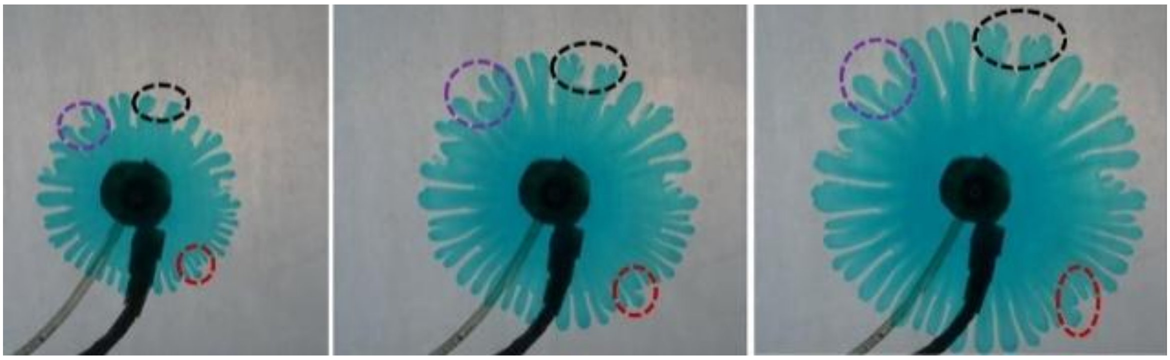

Figure 2
Hele-Shaw cell (Nand et al. 2022)

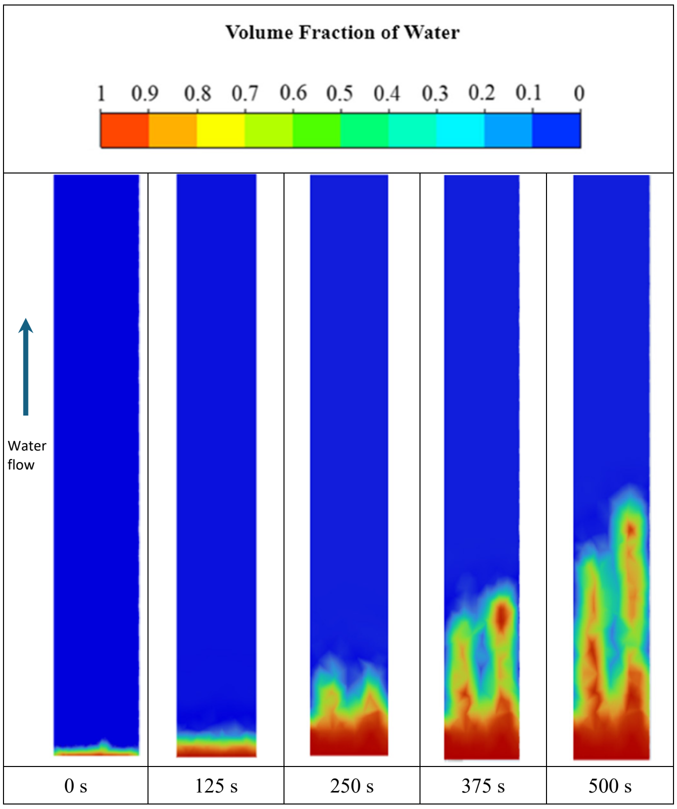

Figure 3
Viscous fingering contours for different times

According to (Homsy 1987), viscous fingering affects transport phenomena by reducing the efficiency of fluid displacement processes and leading to non-uniform flow patterns where a less viscous fluid displaces a more viscous fluid, resulting in the formation of finger-like patterns at their interface, which is the viscous fingering phenomenon itself. Viscosity ratio and capillary number control the dynamics of viscous fingering. Further research has considered the effects of interfacial conditions, viscoelastic/plastic characteristics, geometries, and chemical processes that alter fluid viscosity. The complexity of multiphase flows in porous media prevents their mathematical description.

From Figure 5, it can be seen that the CFD simulation of the current study is much more realistic in comparison with the previous CFD simulation by (Pinilla et al. 2021). Different qualitative behavior is shown by the CFD in comparison to the results given by (Pinilla et al. 2021). According to (Pinilla et al. 2021), the fingers at the core wall had a spike-like morphology and were elongated. However, the fingering patterns identified in Hele-Shaw cells, which have an elongated finger-like pattern with a much longer length than the one from (Pinilla et al. 2021), were more closely resembled by the CFD. Moreover, the non-Newtonian CFD successfully reproduced various VF flow dynamics features such as division, dominant fingers, dendritic-like fingertips, and merging. This phenomenon is attributed to the shear thinning properties present in the non-Newtonian fluid, facilitating the injected fluid's penetration into smaller-radius regions and thereby easing the formation of the viscous finger.

Moreover, features such as the splitting or co-alescence of the fingers' tips are not documented. Once more, the absence of orthogonal faces in a wider range of directions may have significantly impacted the prediction of VF dynamics for the tetrahedral meshes. Furthermore, the prediction of VF dynamics for the tetrahedral meshes could have been notably influenced by the lack of orthogonal faces in various directions.

Additionally, characteristics like the fingers' tip splitting or coalescence, for instance, are not recorded. Again, the lack of orthogonal faces in a broader range of directions could have severely affected the prediction of VF dynamics for the tetrahedral meshes. Once more, the prediction of VF dynamics for the tetrahedral meshes may have been significantly impacted by the absence of orthogonal faces in a wider range of directions.

Pressure contour

The pressure profile and contour clearly indicate that the pressure field within porous material exhibits variations depending on the well's location. The sudden pressure drop that characterizes the pressure field is illustrated in Figure 6 by a shift in color from orange to red at the well's bottom and from green to blue at its top. This contour displays a radial pattern as anticipated. From the profile, it is shown that the pressure experienced a significant amount of pressure drop along the length, starting with an initial pressure of 2.62×10^4 Pa at the length of 0 and reaching the lowest pressure at the length of 0.3 m with a value of 2.03×10^2. Based on (Wilson 2012) research, it is correct that the profile in Figure 7 represents the growth of viscous fingers driven by a positive feedback mechanism. As the local fluid speed increases due to pressure gradients, it becomes more unstable, leading to the formation and growth of viscous fingers. It is also noted that VF occurs at the interface between two fluids of different viscosities and can be driven by pressure gradients. The fluid is compelled to flow in a manner that promotes viscous fingering due to small perturbations at an initially flat interface, generating minor pressure gradients.

The pressure profile also displays the same typical profile of pipeline flows. Additionally, the result of this study demonstrate a noticeable pressure drop along the well until the flow reaches the output.

The pressure profile also exhibits the typical profile of pipeline flows. A quantitative comparison between this generated pressure data and the experimental investigation referred to by (Pinilla et al. 2021) shows a difference of less than 3%. In addition, the results of this study also show a discernible pressure drop down the well until the flow reaches the output.

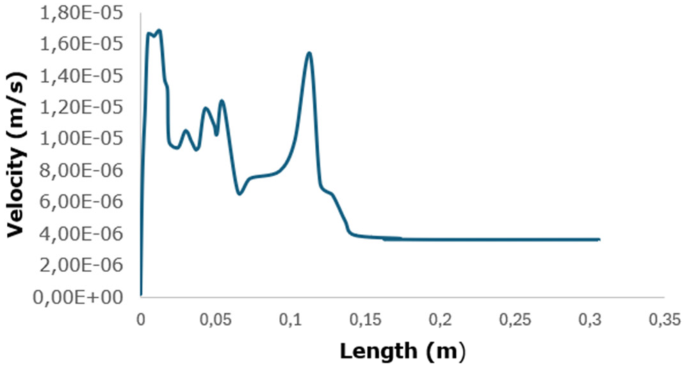

Figure 4
Graph of maximum velocity along the length

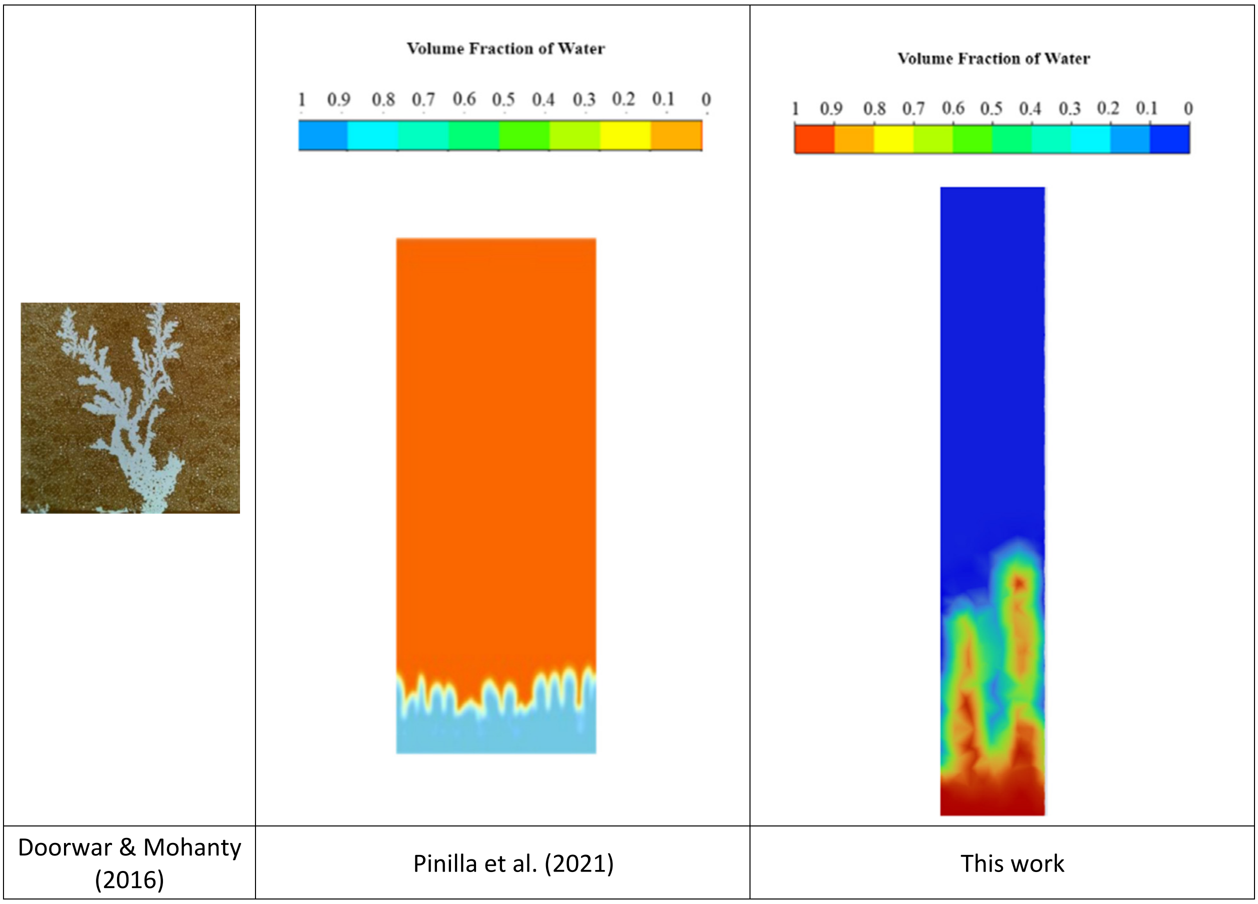

Figure 5
Validation of viscous fingering profile

Porosity

In this study, viscous fingers are simulated using three different porosity values (0.2, 0.5, and 0.7). These values vary in the range of high and ultra-high porosity of a heavy oil field by referring to an experimental work by (J. Zhao et al. 2020). The simulation results indicate that the growth of fingers is significantly influenced by the porosity value. This implies that the existence of porosity in a porous medium can enhance the instability of viscous fingering, with a high porosity value impeding the formation of viscous fingers. From Figure 8, with the same simulation time, the simulation that utilizes the lower porosity value will most likely create the viscous finger more easily than those that have a higher value, where the simulation with a porosity value of 0.7 has not shown any significant pattern of fingering.

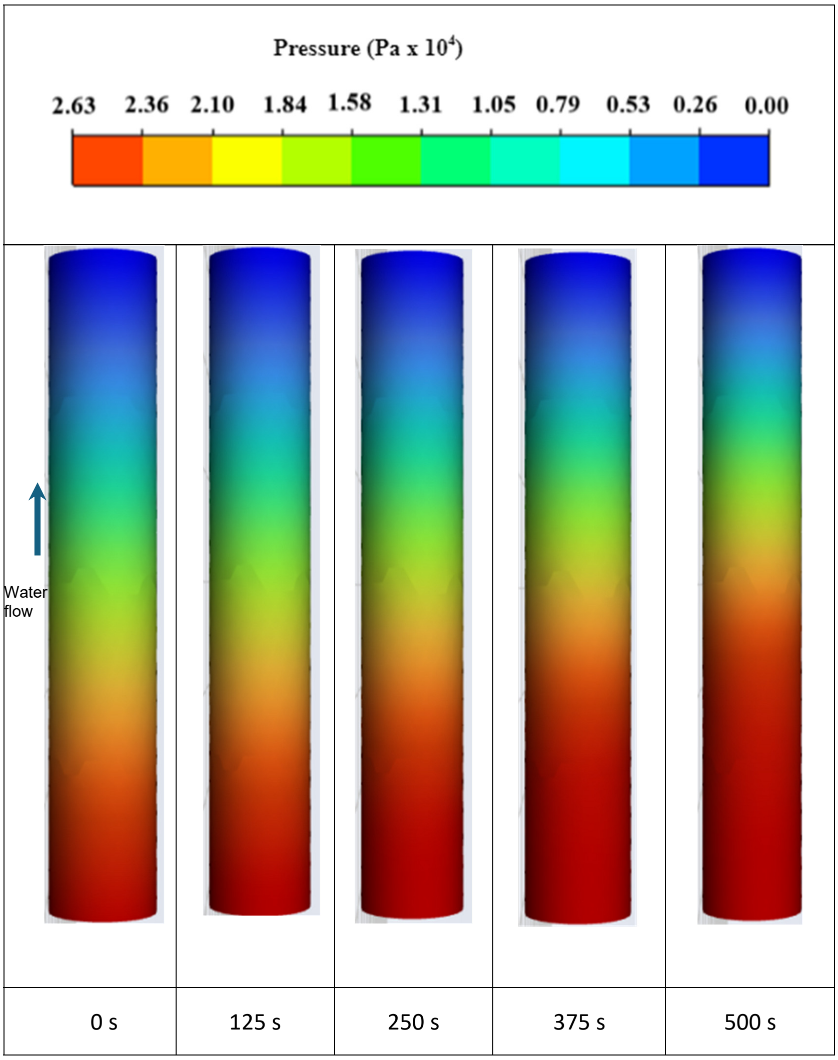

Figure 6
Pressure contour of simulation results for different times

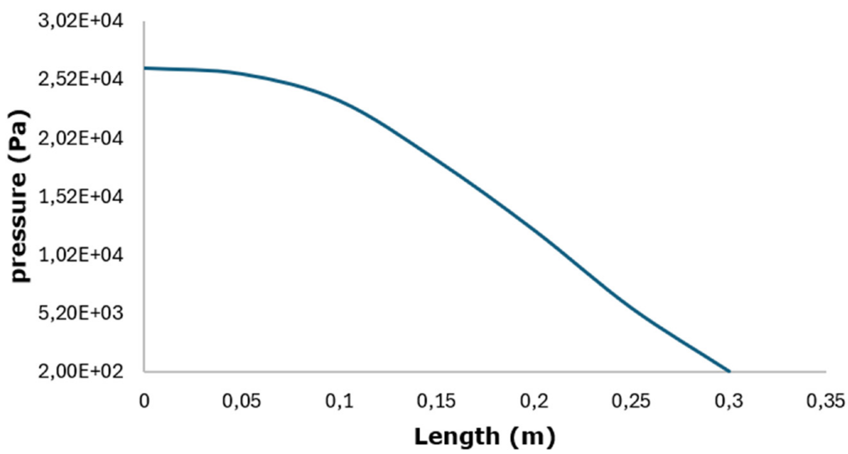

Figure 7
Pressure profile simulation result

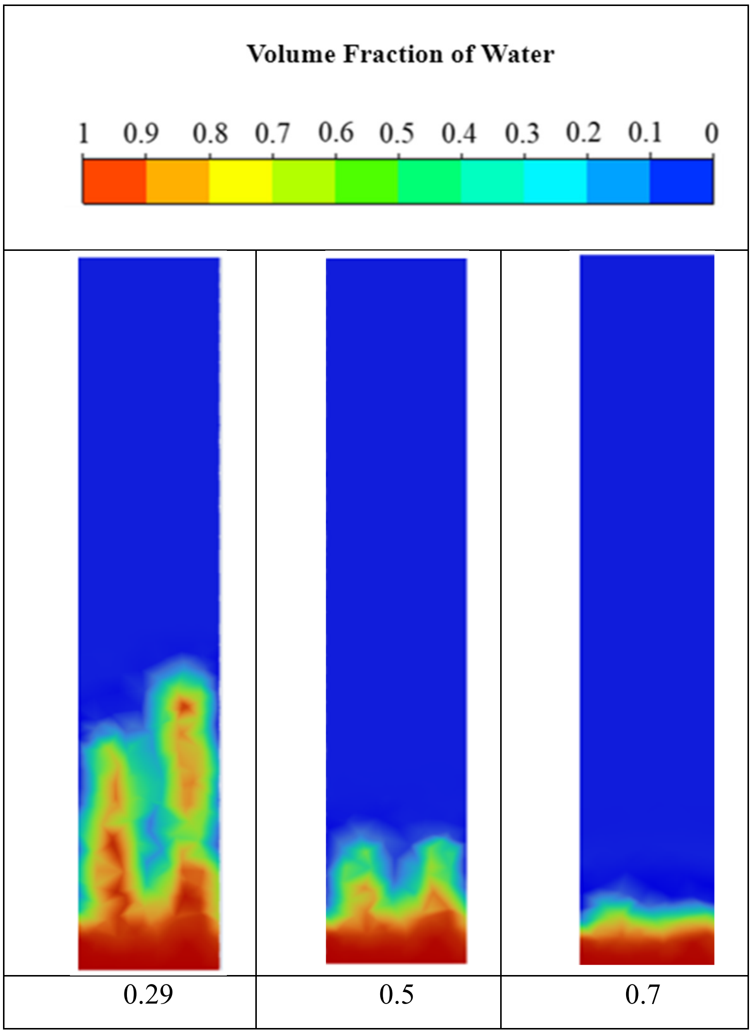

Figure 8
Viscous fingering contours for different porosity values

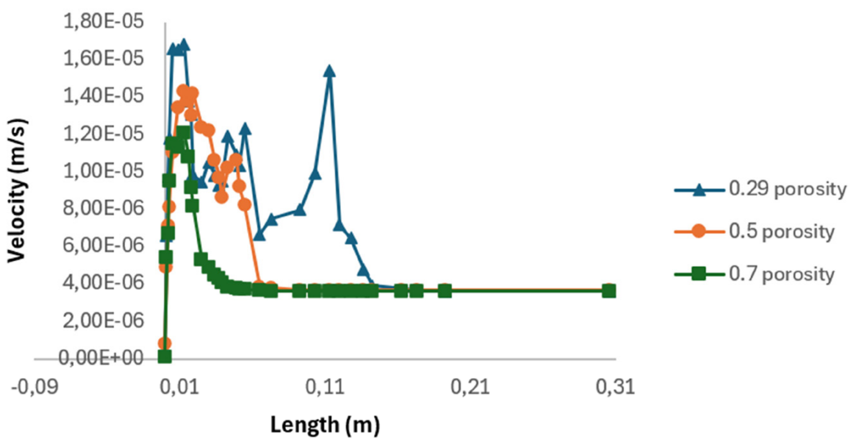

Figure 9
Graph of comparison for maximum velocity for varying porosity

The findings of this study are consistent with the hypothesis put forth by (Sabet et al. 2020), according to which viscous fingering occurs when there are both miscible and immiscible displacements due to unfavorable viscosity gradients. Higher porosity results in increased pore sizes, potentially reducing the viscosity contrast between the fluids and diminishing the adverse viscosity gradient, thereby decreasing the likelihood of viscous fingering. Furthermore, as porosity increases, the fluid flow through the porous medium becomes more intricate, posing challenges for the formation and growth of viscous fingers.

When the porosity is high, the pore sizes increase, which can lead to a less significant difference in viscosity between the two fluids, reducing the adverse viscosity gradient and, consequently, the tendency for viscous fingering. It is also stated that as the porosity increases, the flow of fluids through the porous medium becomes more complex, making it more difficult for viscous fingers to form and grow.

The porosity has some of the most significant impact on velocity due to the porosity's nature in creating fingers. It is illustrated by Figure 9 that lower porosity results in the highest maximum velocity, leading to viscous fingering phenomena. The highest value of velocity for each simulation with different porosity can be seen in Table 2.

Based on Figure 10, it can be concluded that reservoir porosity of the reservoir affects pressure drops during viscous fingering in heavy oil, with higher porosity results in higher pressure drops, aligning this is aligned with the theory by (Pinilla et al. 2021). The simulation with a porosity value of 0.7 shows the highest pressure value at a length of 0 with

Table 2
Comparison of maximum velocity for varying porosity

Porosity	Maximum velocity (m/s)
0.29	1.68×10^5
0.5	1.42×10^5
0.7	1.21×10^5

a value of 3.41×10^4 Pa, followed by 0.5 porosity with a pressure value of 3.15×10^4 Pa, and lastly would be the 0.29 porosity with a value of 2.62×10^4 Pa. The pressure drops in the reservoir can impact the efficiency of heavy oil recovery, with higher pressure drops leading to lower recovery rates. Additionally, reservoir porosity of the reservoir can affect sweep efficiency during waterflooding in oil reservoirs, with lower porosity resulting in more efficient fluid flow and displacement, leading to higher recovery rates.

Kargozarfard, Riazi & Ayatollahi (2018) state that while viscous fingering is known to reduce the efficiency of oil recovery, fingers may enhance sweep efficiency depending on their size and growth pattern. While the growth of a single narrow finger negatively impacts oil displacement efficiency, increasing the number of finger branches and widening them can enhance the areal sweep efficiency. Viscous fingering, an instability phenomenon arising when a less viscous fluid displaces a more viscous one, significantly influences industrial processes like enhanced oil recovery. Hence, comprehending and controlling the effects of viscous fingering is vital for optimizing oil recovery processes in heavy oil reservoirs.

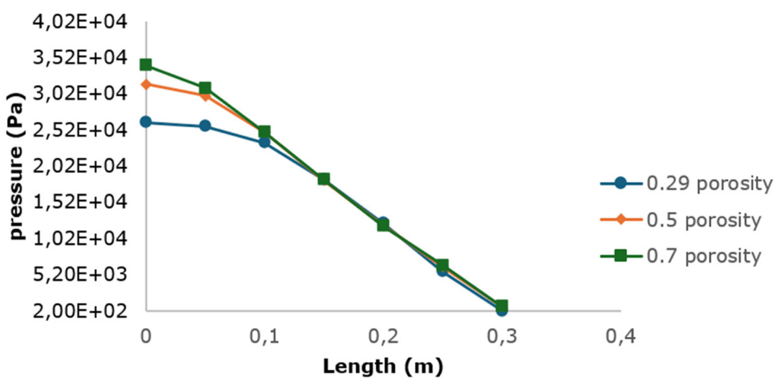

Figure 10
Graph of comparison for pressure for varying porosity

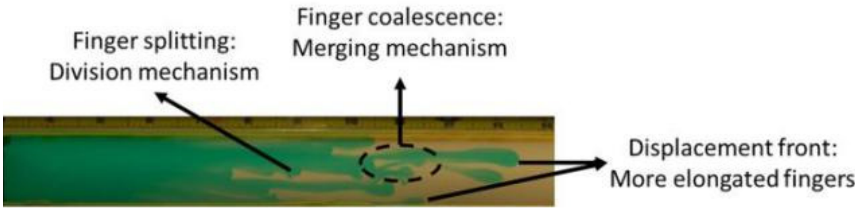

Figure 11
Desired condition of viscous fingering for heavy oil (Malhotra, Sharma & Lehman 2015)

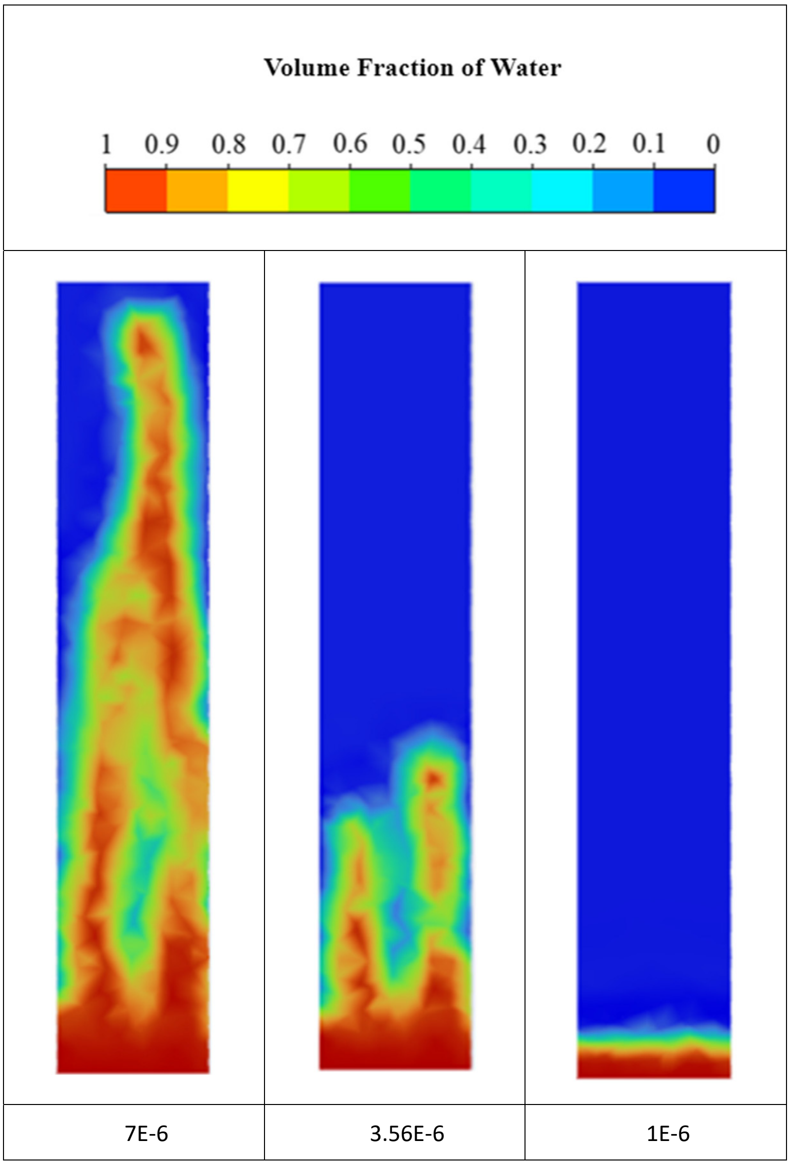

Figure 12
Viscous fingering contours for different injection rates at 500 s

Moreover, the favorable outcomes of viscous fingering CFD simulation in heavy oil production involve replicating the behavior of viscous fingering, a phenomenon resulting from the viscosity ratio between phases. The simulation should aim to replicate the finger pattern, predict severe fingering for water injection into oil, and reproduce displacement regimes; this parameter is illustrated in Figure 11.

Based on Figure 11, it can be inferred that the simulation has met its intended parameter. The simulation results depicted by Figure 8 , particularly for the with porosity value of 0.29, have created a finger splitting trait, which means it has a division mechanism, finger coalescence that is merging, and elongated fingers.

Injection Rate

It can be seen from Figure 12 that increasing the water injection rate could lead to the formation of a much longer and broader viscous finger pattern, while decreasing the water injection rate leads to a slower formation of the viscous finger itself. Furthermore, findings from the experimental study conducted by Kargozarfard, Riazi & Ayatollahi (2018) suggest that injection rate plays a significant role in the appearance and growth of viscous fingers. Lower injection rates lead to the disappearance of fingers before they develop, while higher rates result in longer fingers. This occurs because slower injection rates allow water more time to permeate the pores surrounding the viscous fingers, resulting in their enlargement.

Additionally, results from experimental work by Kargozarfard, Riazi, and Ayatollahi (2018) indicate that the injection rate can influence the appearance and growth of viscous fingers, with lower injection rates causing fingers to disappear before they grow, whereas higher injection rates result in longer fingers. This suggests that there is a possibility of formation. It is also stated by Doorwar and Mohanty (2016) that a lower injection rate will result in a longer time for the viscous finger to form but it will create a much wider finger growth that results in a higher overall recovery although it will take a much longer time. This is because slower injection rates give water more time to seep into the pores around the viscous fingers, causing them to enlarge.

CONCLUSIONS

In conclusion, this study highlights that Non-Newtonian Carreau fluids, with their shear-thinning properties, provide a more accurate and realistic model for simulating viscous fingering phenomena compared to Newtonian fluids. It is concluded that incorporating these fluids into simulations better represents finger formation and dynamics, closely aligning with experimental observations. The study also concludes that porosity plays a significant role in influencing viscous finger development, with lower porosity values (such as 0.29) leading to more pronounced finger splitting, coalescence, and overall formation. Additionally, it is concluded that adjusting injection rates affects finger growth, where lower rates result in wider fingers, enhancing oil recovery. These conclusions offer valuable insights for improving oil recovery efficiency in heavy oil fields by optimizing fluid properties, porosity, and injection rates.

ACKNOWLEDGMENT

This study is fully supported by Process Systems Engineering Laboratory, Department of Chemical Engineering, Faculty of Engineering, Universitas Indonesia

GLOSSARY OF TERMS

Symbols	Definition	Unit
VF	Viscous Fingering	-
CFD	Computational Fluid Dynamics	-
VOF	Volume of Fluid	-
P	Pressure	Pa
U	Velocity	m/s

REFERENCES

Becker, G., C.M. Siefert, R.S. Tuminaro, H. Sun, D.M. Valiveti, A. Mohan, J. Yin & H. Huang, 2018, High-Resolution Viscous Fingering Simulation in Miscible Displacement Using a P-Adaptive Discontinuous Galerkin Method with Algebraic Multigrid Preconditioner. Journal of

Computational Physics 374 (December):495–514. doi:10.1016/j.jcp.2018.07.003.

Cuthiell, D., G. Kissel, C. Jackson, T. Frauenfeld, D. Fisher & K. Rispler, 2006, Viscous Fingering Effects in Solvent Displacement of Heavy Oil. Journal of Canadian Petroleum Technology 45 (07). doi:10.2118/06-07-02.

Di Lullo, Gino & Phil Rae, 2002, New Insights into Water Control - A Review of the State of the Art. All Days, October. doi:10.2118/77963-ms.

Doorwar, Shashvat & Kishore K. Mohanty. 2016. Viscous Fingering Function for Unstable Immiscible Flows. SPE Journal 22 (01):019–031. doi: 10.2118/173290-pa.

González, Diana & Miguel Asuaje, 2014, Simulation of Viscous Fingering Phenomenon Using CFD Tools. ASME 2014 International Mechanical Engineering Congress and Exposition. doi:10.1115/imece2014-36896.

Homsy, G.M., 1987, Viscous Fingering in Porous Media. Annual Review of Fluid Mechanics 19 (1):271–311. doi: 10.1146/annurev.fl.19.010187.001415.

Kargozarfard, Zahra, Masoud Riazi, and Shahab Ayatollahi, 2018, Viscous Fingering and Its Effect on Areal Sweep Efficiency during Waterflooding: An Experimental Study. Petroleum Science 16 (1):105–116. doi: 10.1007/s12182-018-0258-6.

Lei, Timan & Kai H. Luo, 2021, Pore-Scale Simulation of Miscible Viscous Fingering with Dissolution Reaction in Porous Media. Physics of Fluids 33 (3). doi:10.1063/5.0045051.

Luo, Haishan, Mojdeh Delshad, Gary A. Pope, and Kishore K. Mohanty, 2017, Interactions Between Viscous Fingering and Channeling for Unstable Water/Polymer Floods in Heavy Oil Reservoirs. doi:10.2118/182649-ms.

Malhotra, Sahil, Mukul M. Sharma, and Eric R. Lehman, 2015, Experimental Study of the Growth of Mixing Zone in Miscible Viscous Fingering. Physics of Fluids 27 (1). doi:10.1063/1.4905581.

Montes, Daniel, Farid B. Cortés & Camilo A Franco, 2018, Reduction of Heavy Oil Viscosity through Ultrasound Cavitation Assisted by NiO Nanocrystals-Functionalized SiO2 Nanoparticles. DYNA 85 (207):153–160. doi:10.15446/dyna.v85n207.71804.

Moortgat, Joachim, 2016, Viscous and Gravitational Fingering in Multiphase Compositional and Compressible Flow. Advances in Water Resources 89 (March):53–66. doi:10.1016/j.advwatres.2016.01.002.

Nand, Sada, Vandita Sharma, Santanu Kumar Das, Srikant Sekhar Padhee & Manoranjan Mishra. 2022. Effect of Hele–Shaw Cell Gap on Radial Viscous Fingering. Scientific Reports 12 (1). doi:10.1038/s41598-022-22769-x.

Pinilla, Andres, Luis Ramirez, Miguel Asuaje & Nicolas Ratkovich, 2021, Modeling of Viscous Fingering Based on the Numerical Solution of the Navier-Stokes Equations in 3D. Proceedings of the World Congress on Momentum, Heat and Mass Transfer, June. doi:10.11159/icmfht21.lx.201.

Sabet, Nasser, Hassan Hassanzadeh & Jalal Abedi, 2020, Dynamics of Viscous Fingering in Porous Media in the Presence of in Situ Formed Precipitates and Their Subsequent Deposition. Water Resources Research 56 (5). doi:10.1029/2019wr027042.

Shi, Y. & G.H. Tang, 2014, Simulation of Newtonian and Non-Newtonian Rheology Behavior of Viscous Fingering in Channels by the Lattice Boltzmann Method. Computers & Mathematics With Applications 68 (10):1279–1291. doi: 10.1016/j.camwa.2014.08.024.

Singh, Akhileshwar, Krishna Murari Pandey & Yogesh Singh, 2021, CFD Analysis of Viscous Fingering in Hele-Shaw Cell for Air-Glycerin System. Materials Today Proceedings 45 (January):6381–6385. doi: 10.1016/j.matpr.2020.11.069.

Temizel, Cenk, Celal Hakan Canbaz, Minh Tran, Elsayed Abdelfatah, Bao Jia, Dike Putra, Mazda Irani & Ahmad Alkouh, 2018, A Comprehensive Review Heavy Oil Reservoirs, Latest Techniques, Discoveries, Technologies, and Applications in the Oil and Gas Industry. doi:10.2118/193646-ms.

Zhao, J., Zhang, J. & Yang, G., 2020, Feasibility Study on Chemical Flooding in super high porosity and permeability heavy oil reservoir. Journal of Materials Science and Chemical

Engineering, 08(11), 43–53. https://doi.org/10.4236/msce.2020.811004.

Wang, Xiongsheng, Cuicui Yin, Juan Wang, Kaihong Zheng, Zhengrong Zhang, Zhuo Tian &Yongnan Xiong. 2023. Suppressing Viscous Fingering in Porous Media with Wetting Gradient. Materials 16 (7):2601. doi: 10.3390/ma16072601.

Wilson, R. Mark, 2012, Flow Geometry Controls Viscous Fingering. Physics Today 65 (10):15–16. doi: 10.1063/pt.3.1737.

Widarsono, B. et al., 2021, An Integrated Approach for Revisiting Basin-Scale Heavy Oil Potential of the Central Sumatera Basin. Scientific Contributions Oil and Gas, 44(1): 01–20. doi: 10.29017/scog.44.1.493.

Sugihardjo, S., Usman, U. & I, U.P., 2022, Tracer Tests for Heterogeneity Characterization and Saturation Determination on Core Flooding. Scientific Contributions Oil and Gas 33(3): 180–187. doi:10.29017/scog.33.3.821.

Tobing, E.M., 2018, Uji Sensitivitas Konsentrasi Surfaktan Polimer dan Volume Slug Terhadap Perolehan Minyak Melalui Model Simulasi Pola Sumur Injeksi Produksi EOR. Lembaran Publikasi Minyak dan Gas Bumi 52(1) : 1–13. doi:10.29017/lpmgb.52.1.89.